Vol. 34 (2003) ACTA PHYSICA POLONICA B No 8

01072

MEASUREMENT OF CROSS SECTIONS OF HEAVY FRAGMENTS FORMED IN THE INTERACTION OF 0.65–12.7 GeV ^{4}He WITH ^{209}Bi

Z. TODOROVIĆ

Institute of Physics, P.O. Box 68, 11080 Belgrade, Yugoslavia

A. DJORDJEVICH

City University of Hong Kong, 83 Tat Chee Avenue, Hong Kong, China

AND S. SAVOVIĆ

Faculty of Science, R. Domanovića 12, 34000 Kragujevac, Yugoslavia

(Received February 17, 2003; revised version received May 23, 2003)

Formation of heavy fragments in the fission mass region during the interaction with ^{209}Bi of the 0.65, 1.74, 5.1, 8.8 and 12.7 GeV ^{4}He is studied using a sandwich configuration of the Makrofol polycarbonate track detector. Events are analyzed in which at least one heavy fragment is detected. Fragments produced in the experiment are identified and a model-free event-by-event analysis is performed in order to separate different production mechanisms. The cross sections and experimental features are determined for these reaction mechanisms, and so are their variations with the incident energy. Results are compared to the corresponding proton interaction data.

PACS numbers: 25.55.–e, 25.70.Pq, 25.85.–w

1. Introduction

High-energy nucleon or light-ion interactions with heavy nuclei produce a spectrum of reaction products, which suggests the occurrence of a number of competing processes. In such interactions, a significant yield has been observed of slow, heavy fragments with the mass number $A > 40$ [1–6]. Based on their mass number and energy, these fragments are commonly classified into two domains: one for those with A close to the target mass number $A_t (A \gtrsim 2/3A_t)$ and energy $E/A < 0.1$ MeV; and the other for fragments

in the fission mass region $40 < A \lesssim 2/3A_t$ and energy $E/A \approx 0.1 - 0.7$ MeV. Fragments from the former domain are probably formed as residuals in the peripheral cascade-evaporation process after the escape of nucleons or nucleon associations. The latter domain corresponds to a complex mixture of fission fragments (FF) and heavy residue (HR) that results from the de-excitation of highly excited primary target residue through the emission of lower energy particles or intermediate-mass fragments (IMF: $3 \leq Z \leq 20$). A number of possible reaction mechanisms have been considered for production of these fragments, including two modes of fission, deep spallation and fragmentation [2–4, 6–9]. A method of measuring heavy fragments is needed that would improve the ability to distinguish between products originating from different reaction channels.

The main goal of the study being reported is the measurement and analysis of cross sections for the production of heavy fragments in the fission mass region during the interaction of the 0.65–12.7 GeV ^{4}He with ^{209}Bi. Instead of using heavy ions, we use light ones as projectiles in our asymmetric system. Light-ion projectiles are known to provide several important advantages for the study of the nuclear fragmentation processes, including: *(i)* all of the detected fragments are emitted from the target; and *(ii)* the low center-of-mass velocity allows for high-precision measurement of relative velocities and angular correlations. In our experiments, we use Makrofol polycarbonate track detectors in a configuration that allows the correlative measurement of the reaction products with atomic number $Z \geq 8$ in a geometry approaching 4π, and a detail classification of events from different reaction channels.

2. Experimental method

The detectors used in this experiment were two Makrofol foils of the size $(40\times30\times0.2)$ mm^3. As illustrated in Fig. 1, a bismuth target was sandwiched between them by evaporating it onto one of the foils under high vacuum, pressing the other one onto it, and bonding the foils together along two opposite sides using methylchloride. The sandwich packets thus produced were vacuum-sealed in plastic bags to assure contact between the target and foils. The target thickness (which varied from sandwich to sandwich) was between 90 and 130 μg/cm^2 (measurement accuracy 10 percent).

The targets prepared in this manner were exposed to either 0.65 or 1.74 GeV ^{4}He ion beams with normal incidence and flux of 6×10^9 and 4.7×10^{10} alpha particles, respectively, in a Synchrotron machine in Saclay (France). In a Synchrophasotron in Dubna (Russia), additional targets were exposed to 5.1, 8.8 and 12.7 GeV ^{4}He ions with a flux of 8×10^{10} alpha particles. The three flux values were determined with a 10 percent accuracy. They were applied over an area measuring (30×20) mm^2.

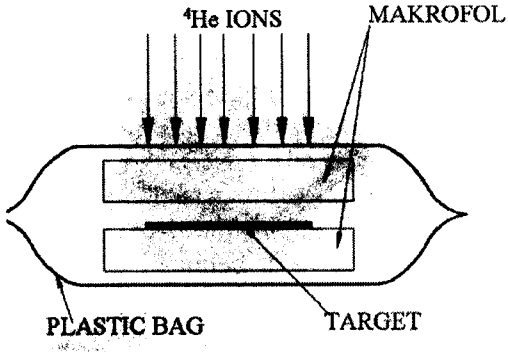

Fig. 1. Detector schematics.

Following the exposition, targets were dissolved by nitrate acid. Each detector was then etched twice in a 20 percent NaOH solution at 60°C over a 25 and 75 minute period, with rinsing in between in water and alcohol (for 25 and 10 minutes, respectively). Agitation by ultrasound was used to aid the reagent diffusion between the Makrofol foils during the target dissolution, track etching and rinsing in water and alcohol. For IMFs $8 \leq Z \leq 20$ and $10 < \text{REL} < 23$ MeV mg^{-1} cm^2, (REL stands for Restricted Energy Losses), the difference between the track portions etched during the first and second round of etching was visible. This simplified the fragments' parameter identification (mean track etch rate and the total range). Thus, we were able to identify the energy and charge of the IMFs with a charge resolution of $\Delta Z \leq 1$ [10,11].

A record of tracks (after the second round of etching) is shown in Fig. 2 for an event with one IMF and one heavy fragment produced by the interaction of the 8.8 GeV ^{4}He with ^{209}Bi. For the track pertaining to the IMF, the difference between the sections developed during different rounds of etching is evident. The tracks formed by heavy fragments with $Z > 20$ could easily be recognized because of their high etch-rate. They were almost fully developed after the first etching. Their mass and energy were determined from the empirical energy-range $E = f(R)$ and mass-range $A = f(R, E)$ relations [11]. The uncertainty limits are approximately 10 u and 10 MeV, respectively.

Once etched, detector foils were reassembled together with a graduated mesh. They were vacuum-resealed in plastic bags in order to restore their original configuration. Detectors were then scanned and track parameters were measured under the optical magnification of a microscope of 300×, and 900×, respectively. The scanning revealed events with one track each (disassociated from other tracks) and also events with two, three or four tracks intersecting in the planes of the respective targets (which indicated

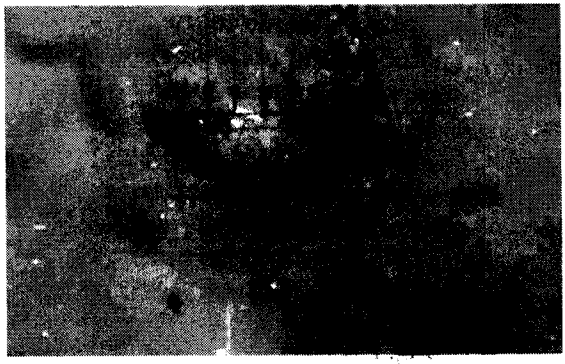

Fig. 2. Record of an event with one IMF and one heavy fragment (8.8 GeV ^{4}He+^{209}Bi) after the second etching.

that each such group of tracks was formed by fragments from one and the same interaction).

For detectors of the type deployed in this study, it is necessary to introduce a correction for the number of events observed. The reasons for this include *(i)* the inability to detect fragments at angles beyond critical, and *(ii)* the coincidence of events of different type. Absorption of the fragments by the ^{209}Bi target could also be considered in principle, but for the target thickness below 130 μg/cm^2 a loss of less than one percent of fragments occurs, which was neglected. Critical angles (for the cause *(i)* above) were evaluated based on the experimentally obtained angular distribution of energy for the reaction products, which was then used to estimate the detection efficiency during scanning: 90–95 percent for heavy fragments and 80–90 percent for IMFs. The coincidence of two single tracks (cause *(ii)* above) or of a single track and a binary event may lead to false binary or ternary events, respectively. The frequency of occurrence of such coincidences has been calculated assuming a Poisson distribution for the spatial distribution of the reaction events. Percentages for the double and triple random coincidences were thus estimated at 0.05–0.2 and 2–5 percent of the respective numbers of times these events were observed.

3. Results and discussion

All observed target products were identified and events from different reaction channels were classified. Events with a heavy residue were characterized by the presence of only one heavy fragment $Z > 20$ or groups with one heavy fragment and one or more IMFs ($M_H = 1$ events). Cases with

only one heavy fragment in the range $R \leq 5\mu$m were not analyzed because they were much less clearly defined. Based on the range-energy dependence for these fragments in Makrofol [12], it was determined that their energy was $E/A < 0.1$ MeV. Representing residuals with mass number A close to the target mass number $A_t (A \gtrsim 2/3A_t)$, the most of these fragments were probably formed in the peripheral cascade-evaporation process after the escape of nucleons or nucleon associations [13]. The fission events with two heavy fragments ($Z > 20$) were included irrespective of whether coincident IMFs ($8 \leq Z \leq 20$) existed ($M_H = 2$ events). In Table I is given the number of the analyzed events where one ($M_H = 1$), two ($M_H = 2$) and three ($M_H = 3$) heavy fragments $Z > 20$ are registered, and the total number of events.

TABLE I

The number of events studied in different event categories and the total number of events for projectile energies used.

E (GeV)	0.65	1.74	5.1	8.8	12.7
$M_H = 1$	328	857	1520	2808	2589
$M_H = 2$	1641	1632	1751	2588	1961
$M_H = 3$	–	12	35	102	91
Total	1969	2501	3306	5498	4641

Mass and energy distributions are shown in Fig. 3 for heavy fragments produced in the events with $M_H = 2$ and $M_H = 1$ in the 8.8 GeV ^{4}He+^{209}Bi interaction. It can be observed that the mass distribution of heavy fragments for $M_H = 1$ events is in the range of fission fragment masses. This agrees with earlier reported mass and energy distributions for heavy fragments in the fission mass region [1–7] which were determined by different techniques for monitoring interactions of high-energy nucleon and light-ion projectiles with heavy nuclei. Ternary events with three correlated heavy fragments ($M_H = 3$) contributed to less than 2 percent of the total number of events and were not analyzed further for lack of reliable statistics.

It was observed that the multiplicity of intermediate mass fragments for events with one heavy fragment ($Z > 20$) varied from 0 to 3. Events with multiplicity $M_{IMF}^{obs} = 0$ were produced mainly in deep spallation and fragmentation processes in which IMFs were emitted with energy below the detector threshold. Events in which one heavy fragment was emitted in correlation with IMFs, have originated from the fragmentation processes. The number of events in which at least one IMF was detected in addition to one heavy fragment, varied from 10 percent (at 0.65 GeV) to 29 percent (at 12.7 GeV) of the number of events with $M_H = 1$. The mean values of the multiplicity of IMFs in these events increased from 1.06 (at 0.65 GeV) to 1.19 (at 12.7 GeV).

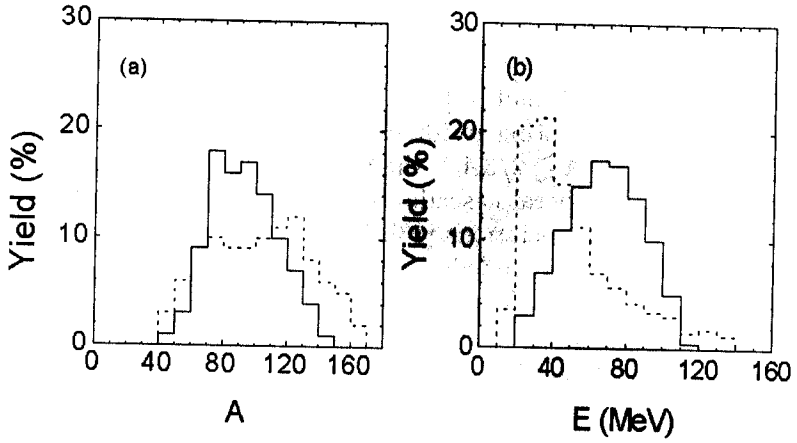

Fig. 3. Distribution of (a) mass and (b) energy of heavy fragments produced in events with $M_{\mathrm{H}} = 1$ (dotted line) and $M_{\mathrm{H}} = 2$ (solid line) in the 8.8 GeV ^{4}He+^{209}Bi reaction.

Event cross sections were calculated using the expression $\sigma_i = F_i/NP$, where: F_i was the number of events of a given type per cm^2; N was the number of target atoms per cm^2; and P was the number of incident particles per cm^2. Calculation uncertainties are due to the statistical and scanning errors, uncertainties in the thickness of the target layers, and errors in estimating the flux. As a function of the incident energy, cross sections are shown in Fig. 4 for production of single heavy fragments ($M_{\mathrm{IMF}}^{\mathrm{obs}} = 0$) and heavy fragments in correlation with IMF. For the interactions 1.8–4.4 GeV ^{3}He+Ag, Au, it has been reported previously [14] that the Z-distribution of IMFs decreases rapidly with increasing Z. Therefore, one should expect a larger number of events with emission of heavy residue $M_{\mathrm{IMF}}^{\mathrm{obs}} = 0$ in correlation with IMF with $Z < 8$. The similarity of the curves in Fig. 4 leads us to conclude that not only the deep spallation but also the fragmentation processes play an important role in the formation of the heavy residue. Measured as a function of the ^{4}He energy, total cross sections for production of events with $M_{\mathrm{H}} = 1$ are shown in Fig. 5 together with the corresponding proton interactions data [15,16] obtained using a mica track detector. These cross sections may be compared because the mica track detector is sensitive for fragments with $Z \geq 15$ and in these proton interactions heavy single fragments with projected track length greater than 4 μm [15] and 2 μm [16] have been analyzed. One can observe in Fig. 5 that the cross sections for production of heavy residue rise in a similar manner with the projectile energy for both ^{4}He+^{209}Bi and p+^{209}Bi interactions. However, the former are about 1.5 times greater.

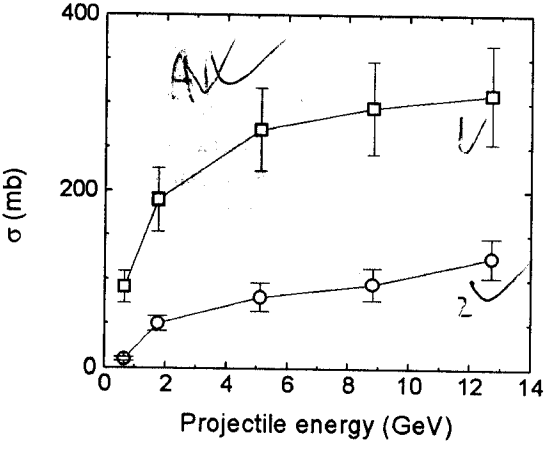

Fig. 4. Cross sections for the production of events with a single heavy fragment (squares) and heavy fragment in correlation with IMF (circles) as a function of incident energy in the ^{4}He+^{209}Bi reaction. Lines are drawn for visual aid.

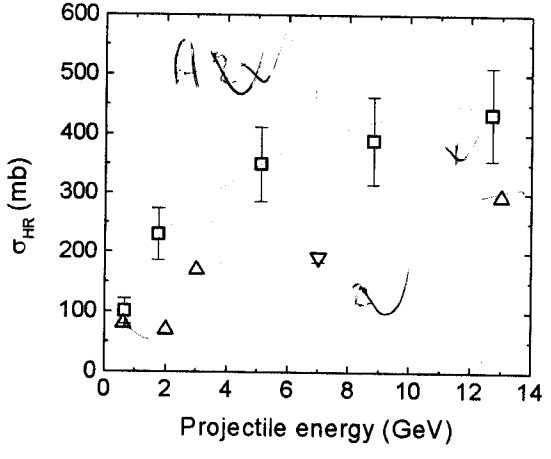

Fig. 5. Cross sections for the production of heavy residues in the ^{4}He+^{209}Bi reactions: □ — present work and p+^{209}Bi: △ — [15]; ▽ — [16].

Fission events were characterized by the presence of two heavy fragments in correlation, irrespective of the existence of coincident IMFs ($8 \leq Z \leq 20$). The number of events with at least one detected IMF in addition to two heavy fragments varied from 0.5 percent (at 1.74 GeV) to 6 percent (at 12.7 GeV) of the number of all fission events. The mean value of the multiplicity for these events was approximately 1.05. It did not vary much with the projectile energy.

Fission events with $M_{\rm IMF}^{\rm obs} = 0$ can be produced by two different mechanisms [3,6]. One of them is thermal binary fission. Coincidence studies with relativistic light-ion beams show that thermal binary fission events are observed primarily for peripheral interactions and are associated with low multiplicities of neutrons and light charged particles. The other mechanism is violent. In violent collisions, the statistical deexcitation through emission of a number of neutrons and light charged particles or IMFs that cannot be detected in Makrofol follows the formation of the hot composite system and the fission occurs at the end of the evaporation chain. In order to distinguish thermal binary fission events from events with $M_{\rm IMF}^{\rm obs} = 0$ in which two heavy fragments are produced after more violent collisions, we used the dependence $\nu_{ij}(\Delta A)$, where: ΔA is a difference between the target mass and the sum of the heavy fragment masses, and ν_{ij} is the relative velocity between fission fragments. Two clearly separated clusters can be observed in the $\nu_{ij}(\Delta A)$ graph in Fig. 6 for the 8.8 GeV ^{4}He+^{209}Bi interaction. For events with $\Delta A < 30$, a narrow distribution of relative velocities is centered at a value which corresponds to Viola systematics [17] characterizing the thermal binary fission processes. For larger ΔA, the ordinate shifts upwards and its distribution broadens significantly presumably because of the emission of a number of neutrons and light charged particles as well as the emission of IMF with $Z < 8$. These events, together with those with at least one IMF registered in addition to two heavy fragments, form a group of fission events produced after violent collisions.

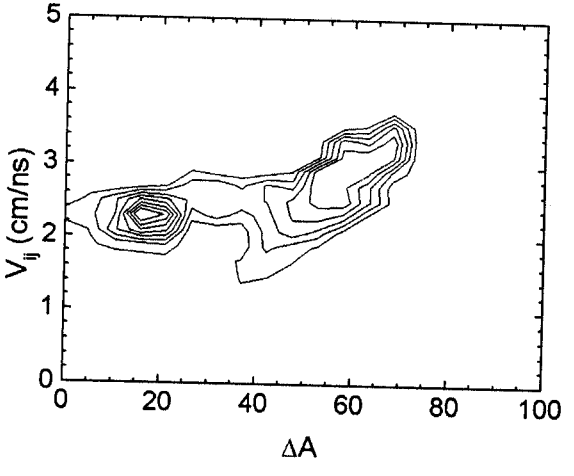

Fig. 6. Contour plot of the relative velocity between fragments for $M_{\rm IMF}^{\rm obs} = 0$ events as a function of the mass loss for the 8.8 GeV ^{4}He+^{209}Bi reaction.

For events with $M_{\mathrm{IMF}}^{\mathrm{obs}} = 0$ produced either in thermal fission or violent collisions, folding angle (θ_{ff}) distributions are shown in Fig. 7 for the 0.65, 1.74, 5.1 and 8.8 GeV ^{4}He+^{209}Bi interactions. The angles were determined from directional unit vectors ($\underline{f}$) of the two fission fragments: $\theta_{ff} = \arccos(\underline{f}_1 \cdot \underline{f}_2)$. For fission events produced in violent collisions, one can observe in Fig. 7 that the folding angle distribution broadens towards smaller angles and its maximum decreases with increasing projectile energy. This reflects the importance of the linear momentum transfer and the increasing influence of the particle emission (particularly IMFs with $Z < 8$) prior to the fission process. The distributions pertaining to thermal fission processes peak around 170–175° and do not change significantly with the projectile energy.

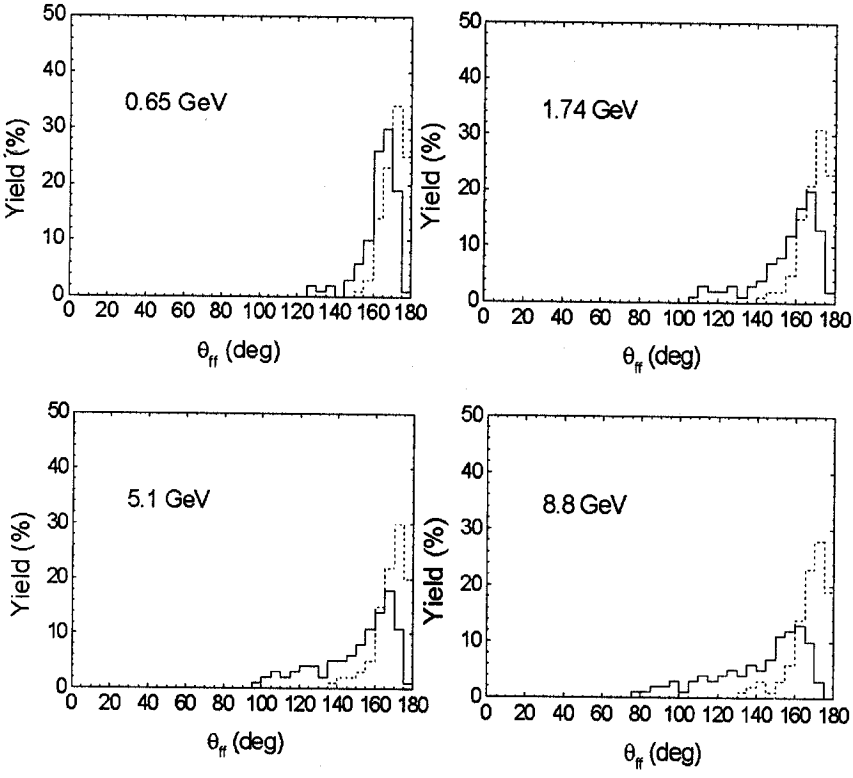

Fig. 7. Folding angle θ_{ff} distributions for events with $M_{\mathrm{IMF}}^{\mathrm{obs}} = 0$ produced in thermal fission processes (dotted line) and violent collisions (solid line) in the ^{4}He+^{209}Bi reaction.

As a function of the incident energy, cross sections are shown in Fig. 8 for production of thermal fission events and fission events in violent collisions. One can observe that the cross section for the former decreases rapidly to about 3 GeV and slower further on. Conversely, the cross section for the latter initially increases rapidly up to about 3 GeV, slower further on, and decreases thereafter. The high gradients for energies up to 3 GeV can be understood in terms of the enhanced energy deposition provided by the excitation of Δ resonances during the cascade, followed by reabsorption of decay pions [14]. Above about 2 GeV, the cross sections for production of fission events in violent collisions are larger than those for thermal fission. This is due to the rise in the incident energy as the collisions become increasingly violent and only in more peripheral collisions is the excitation sufficiently week for the thermal fission to occur. Moreover, in the violent process following a significant emission of neutrons and charged products, residual nuclei are produced with a mass in the domain of light nuclei. For them, the fission probability depends on the excitation energy of the residual nuclei (not on the fissility parameter) [6].

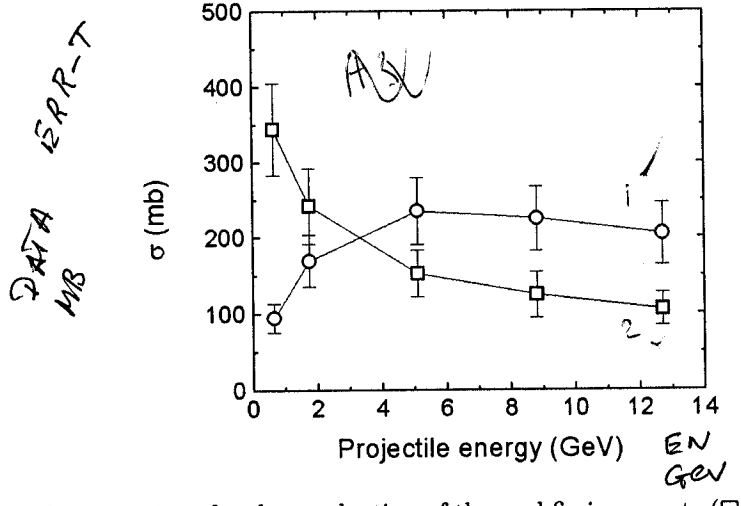

Fig. 8. Cross sections for the production of thermal fission events (□) and events in violent collisions (○) as a function of the incident energy in the ^{4}He+^{209}Bi reaction. Lines are drawn for visual aid.

Measured total cross sections for production of fission events ($M_H = 2$) are shown in Fig. 9 together with the corresponding proton interactions data [15,16,18] obtained using the mica track detector. With increasing projectile energy, the decrease of the cross section for the fission of ^{209}Bi in interactions with protons is similar to the same for interactions with ^{4}He. However, the absolute magnitudes are about 1.6 times greater for the latter.

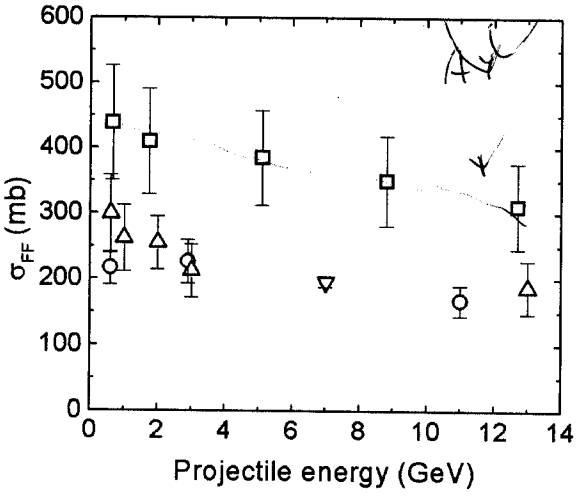

Fig. 9. Cross sections for the production of fission events in the reactions ^{4}He+^{209}Bi: □ — present work and p+^{209}Bi: △ — [15]; ▽ — [16]; ○ — [18].

Results obtained for ^{4}He+^{209}Bi interactions show that the fission mode weakens while the cross section for heavy residues increases with increasing bombarding energy. A relative measure between the heavy residue formation and production of fission events may be expressed by the ratio of the respective cross sections: σ_{HR}/σ_{FF}. Based on data presented in Fig. 5 and Fig. 9, the ratio σ_{HR}/σ_{FF} equals 0.23, 0.56, 0.9, 1.1 and 1.39 for the projectile energies of 0.65, 1.74, 5.1, 8.8 and 12.7 GeV, respectively. The increase of σ_{HR}/σ_{FF} with projectile energy can be attributed to the increase in the excitation energy of the primary reaction residue. As the mean excitation energy rises, so does the probability of production of lower energy particles and IMFs, which reduces the amount of the primary reaction residue and excitation energy. Consequently, fission decay is inhibited, extending the survival of the heavy residue.

4. Conclusion

We have studied the production of heavy fragments in fission mass region in the interactions of 0.65, 1.74, 5.1, 8.8 and 12.7 GeV ^{4}He with ^{209}Bi. Based on our measurement of the target fragments with $Z \geq 8$, we have observed dominant mechanisms for production of heavy residue and fission fragments. It has been shown that the heavy residues are produced in deep spallation and fragmentation processes. Significant differences were observed between the IMF emission associated with fission and that associated with

the heavy residue, indicating that the IMF emission plays an important role in the survival of the latter. By correlating observed characteristics of fission events, we have identified and separated events originating from thermal and more violent processes. Above about 2 GeV, cross sections for production of fission events in violent collisions are larger than those for thermal fission events. It has been shown that the cross sections for heavy residues increase and those for the production of fission events decrease with increasing projectile energy. The relative ratio of the corresponding cross sections (σ_{HR}/σ_{FF}) is greater than unity for projectile energies in excess of about 5 GeV. This effect is attributed to the rise in the emission of neutrons and charged products at higher projectile energies, leading to a less fissile primary reaction residue.

We are grateful to Prof. A. M. Baldin and Prof. N. Semenyuskin for exposing our detectors and measuring the flux. We are also thankful to the technical staff of our Laboratory for their dedication and painstaking measurement. This work was supported by the Serbian Ministry of Science, Technology and Development under Grant No. 1488.

REFERENCES

[1] P. Kozma, A.I. Malakhov, *Phys. Lett.* **B305**, 399 (1993).

[2] M. Gloris, R. Michel, F. Sudbrock, U. Herpers, P. Malmborg, B. Holmqvist, *Nucl. Instrum. Methods* **A463**, 593 (2001).

[3] P.L. McGaughey, W. Loveland, D.J. Morrissey, K. Aleklett, G.T. Seaborg, *Phys. Rev.* **C31**, 896 (1985).

[4] W. Loveland, Cheng Luo, P.L. McGaughey, D.J. Morrissey, G.T. Seaborg, *Phys. Rev.* **C24**, 464 (1981).

[5] G. Klotz-Engmann, H. Oeschler, J. Stroth, E. Kankeleit, Y. Cassagnou, M. Conjeaud, R. Dayras, S. Harar, R. Legrain, E.C. Pollacco, C. Volant, *Nucl. Phys.* **A499**, 392 (1989).

[6] J. Hüfner, *Phys. Rep.* **125**, 129 (1985).

[7] A.I. Warwick, H.H. Wieman, H.H. Gutbrod, M.R. Maier, J. Peter, H.G. Ritter, H. Stelzer, F. Weik, M. Freedman, D.J. Henderson, S.B. Kaufman, E.P. Steinberg, B.D. Wilkins, *Phys. Rev.* **C27**, 1083 (1983).

[8] E.C. Pollacco, J. Brzychczyk, C. Volant, R. Legrain, R.G. Korteling, D.S. Bracken, K. Kwiatkowski, K.B. Morley, E. Renshaw Foxford, V.E. Viola, N.R. Yoder, H. Breuer, J. Cugnon, *Phys. Lett.* **B482**, 349 (2000).

[9] V. Aleksandryan, J. Adam, A. Balabekyan, A.S. Danagulyan, V.G. Kalinnikov, G. Musulmanbekov, V.K. Rodionov, V.I. Stegailov, J. Frana, *Nucl. Phys.* **A674**, 539 (2000).

[10] Ž. Todorović, R. Antanasijević, *Nucl. Instrum. Methods.* **212**, 217 (1983).

[11] D.L. Lazić, Ž. Todorović, *Nucl. Instrum. Methods* **B61**, 239 (1991).

[12] J. Tripier, G. Remy, J. Ralarosy, M. Debeauvais, R. Stein, D. Huss, *Nucl. Instrum. Methods* **115**, 29 (1974).

[13] Ž. Todorović, S. Savović, S. Jokić, *Eur. Phys. J.* **A2**, 295 (1998).

[14] E. Renshaw Foxford, K. Kwiatkowski, D.S. Bracken, K.B. Morley, V.E. Viola, N.R. Yoder, C. Volant, E.C. Pollacco, R. Legrain, R.G. Korteling, W.A. Friedman, J. Brzychczyk, H. Brener, *Phys. Rev.* **C54**, 749 (1996).

[15] J. Hudis, S. Katcoff, *Phys. Rev.* **C13**, 1961 (1976). — 00644

[16] H.A. Khan, N.A. Khan, *Phys. Rev.* **C29**, 2199 (1984). — 00611

[17] V.E. Viola, K. Kwiatkowski, M. Walker, *Phys. Rev.* **C31**, 1550 (1985).

[18] R. Brandt, F. Carbonara, E. Cieslak, H. Piekarz, J. Piekarz, J. Zakrzewski, *Rev. Phys. Appl.* **7**, 243 (1972). — 00605